LAWRENCE
LIVERMORE
NATIONAL
LABORATORY

UCRL-TR-206331

Measurements of an ARS DE204S Cryocooler's Thermal and Vibration Characteristics

Benjamin Haid

September 1, 2004

Disclaimer

This document was prepared as an account of work sponsored by an agency of the United States Government. Neither the United States Government nor the University of California nor any of their employees, makes any warranty, express or implied, or assumes any legal liability or responsibility for the accuracy, completeness, or usefulness of any information, apparatus, product, or process disclosed, or represents that its use would not infringe privately owned rights. Reference herein to any specific commercial product, process, or service by trade name, trademark, manufacturer, or otherwise, does not necessarily constitute or imply its endorsement, recommendation, or favoring by the United States Government or the University of California. The views and opinions of authors expressed herein do not necessarily state or reflect those of the United States Government or the University of California, and shall not be used for advertising or product endorsement purposes.

This work was performed under the auspices of the U.S. Department of Energy by University of California, Lawrence Livermore National Laboratory under Contract W-7405-Eng-48.

Measurements of an ARS DE204S Cryocooler's Thermal and Vibration Characteristics

Ben Haid
NIF Cryogenic Target System
Engineer
Lawrence Livermore National Laboratory
Livermore, California
August 23, 2004

This document describes measurements that characterize an Advanced Research Systems DE204S cryocooler system. The data is relevant to the thermal performance and vibration characteristics of the cold-head. The thermal measurements include heat load mapping of the 1st and 2nd stage, and temperature fluctuation measurement of the 2nd stage heat station. A comparison of fluctuation measurements by four different sensors is also included to support the 2nd stage fluctuation results. Finally, optical measurement of the cyclic 2nd stage heat station deflection is described.

1st and 2nd Stage Mapping

We have created a load map for this cryocooler system because the manufacturer does not provide one that covers the range of 1st stage heat load that is expected in NIF's Mk-1 cryogenic target system. The cryocooler cold-head, shown in Figure 1, was set-up as illustrated in Figure 2. A heater and a silicon diode temperature sensor are attached to each heat station. A copper shield encloses the 2nd stage and is cooled by the 1st stage. The shield is covered with ten layers of crinkled aluminized mylar film. Temperature is recorded while various heat loads are applied to the stages. The 1st stage sensor is accurate to within 1K at room-temperature and below. The 2nd stage sensor is accurate to within 0.5K for temperatures below 100K, and 1K for temperatures above 100 K.

The green stars of Figure 3 indicate steady-state temperatures that are measured for various combinations of 1st and 2nd stage heat loads. The blue curves indicate lines of constant 1st stage heat load (vertical) or 2nd stage heat load (horizontal) that are approximated using 2-D linear interpolation. The curve that represents a 0 W 1st stage heat load agrees well with the manufacturer's typical refrigeration curve of Figure 4. Figure 5 shows the map extended close to room temperature for both the 1st and 2nd stage temperature axes.

2nd Stage Temperature Fluctuations

The cryocooler implements the G-M cycle at 2.4 Hz when powered with a line frequency of 60 Hz AC. The temperature of the 2nd stage fluctuates as a result of the reciprocating processes that comprise this cycle. Experiments have shown that the 2nd stage fluctuations can exceed 1 K peak-to-peak. Since the Mk-1 is required to provide temperature stability of better than 100 mK peak-to-peak, the Mk-1 design must include a means of attenuating these fluctuations.

The 2nd stage temperature was recorded at a fast enough rate to reveal the cyclic temperature fluctuations. A silicon diode is mounted to the cryocooler 2nd stage, using the mechanical clamping method illustrated in the photograph of Figure 7a. The diode is enclosed within a rectangular hermetic package as supplied by the manufacturer (Lake Shore P/N DT-470-SD). A screw compresses 2 belleville washers that press the sensor against the contact surface. A thin layer of Apiezon-N grease is applied to the contact surface prior to mounting the sensor.

Figures 6a,b,&c show temperature traces at ≈5K, 10K, and 20K. The fluctuations for the 10K measurement are the largest of the 3 and are on the order of 1.5K peak-to-peak. The fluctuation versus temperature trend and the shape of the fluctuation agree well with what has been reported for another 4K G-M cycle cryocooler that was manufactured by Sumitomo Heavy Industries, Ltd [1]. The fluctuation magnitude is largest when operating just above 10K.

Sensor Comparison

We tracked temperature fluctuations using several sensors simultaneously to verify that we have measured the magnitude of the cryocooler's 2.4 Hz-fluctuations with reasonable accuracy. 4 sensors are mounted at one end of a cold-worked OFHC copper rod as shown in Figure 8. The sensors are located 90° apart on the rod's circumference. The rod is mounted to a cryocooler 2nd stage. The large length to diameter ratio of the rod ensures a nearly uniform temperature around the circumference, and therefore among the sensor locations. The temperature fluctuations propagate along the rod and calculations shown that they are only moderately attenuated when they reach the sensors.

A different combination of sensor model and mounting technique is used with each sensor. The various combinations are shown photographically in Figure 7: (a) a silicon diode (Lake Shore part no. DT-470-SD-12A) in a hermetic package and mounted in the same way as described in the previous section, (b) a Cernox chip (CX-1070-SD) with the same style packaging and mounting as the diode, (c) a bare Cernox chip (XCX-1070-BC-HT-4L-92) that was mounted directly to the copper rod with 52% In / 48% Sn solder, and (d) a bare Cernox chip (CX-1070-BC) that was adhered directly to the copper with Glyptal 1202 varnish.

The temperature of each sensor is recorded at 1000 Hz using isolated voltage inputs of a National Instruments DAQPad-6020E data acquisition system, indicated in Figure 8. Each sensor is excited with its own 10 μA current source. Calibration curves are used for converting the resistance across the Cernox sensors to temperature. The calibration accuracy of Cernox sensors is typically ±6 mK at 10 K and ±5 mK at 4.2 K. The diode voltage drop is converted using a standard curve.

The Cernox temperature traces at ≈7.5 K are shown in Figure 9. The soldered and clamped sensors agree very well, but attenuation and lag is observed with the varnish mounted chip, probably due to the very low thermal conductivity of the varnish at this temperature. Figure 10 shows the same traces along with the diode measurement. There is significant difference in the absolute temperature measurement because this sensor is only accurate to within 0.5 K, but the magnitude and shape of the fluctuations agree very well with the soldered and clamped Cernox sensors. Comparable agreement among the sensors is also observed at 5, 10, and 15 K. The close agreement indicates that the temperature fluctuation magnitudes measured using a clamped silicon diode is reasonably accurate.

Comparison of Sensor Measurements [2]

The Mk-1 cryostat must allow for stable positioning of the target. The cryocooler 2nd stage heat station sustains cyclical displacements at the same frequency as the refrigeration cycle. The displacements have been measured to determine if it is suitable to mount targets directly to the cryocooler 2nd stage heat station, or if some intermediate mechanical isolation is required.

A camera was set up to observe the motion of the cryocooler heat station in a plane that includes the cryocooler axis, as shown in the photograph of Figure 11. A long distance microscope lens focuses the camera on a resolution target. The target is located at the end of an 8” rod mounted to the cryocooler 2nd stage. The rod positions the target where it can be viewed through the vacuum chamber view port.

The camera captures images at a rate of 30 frames/s and a resolution of 2 μm. The 2nd stage motion is recorded while operating at the lowest achievable of 8 K. The lowest temperature is higher for this test than for others because no radiation shields are installed. Deflections of 14 μm peak-to-peak are observed for the z-direction (refer to Figure 2 for coordinate definition) and 12 μm peak-to-peak for the r-direction, resulting in a total displacement in the camera plane of view of 18±4 μm peak-to-peak. Most of the 4 μm uncertainty is a result of relative motion between the camera and the vacuum chamber. If the deflection normal to the plane of view is comparable to the r-directed deflection, then the total deflection is 22±6 μm.

Upon shutting the cryocooler off, the 2nd stage heat station immediately settles to within 4 μm of the final rest position, and then drifts to the final rest position over a period of about 2 s. The cryocooler was shut-off and restarted six times to test the consistency of the final rest position. The change in final rest position was less than the observational limits of the measurement system.

References

[1] Rui L et al., “A simple method of temperature stabilization for 4 K GM cryocooler.” *Proceedings of the Sixteenth International Cryogenic Engineering Conference,* v.1 pp.355-8 (1997)
[2] Measurements originally performed and documented by Clark Radewan, Johnson Controls World Services Inc.

Figures

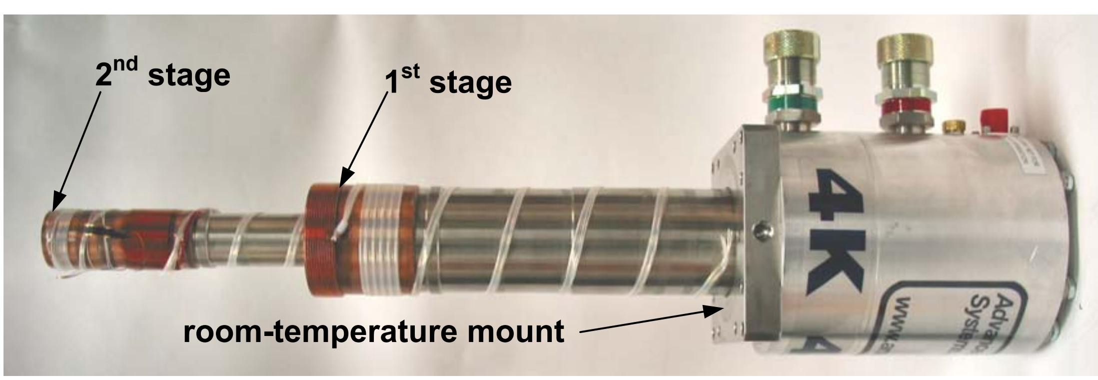

Figure 1: Photograph of the ARS DE204S cold-head.

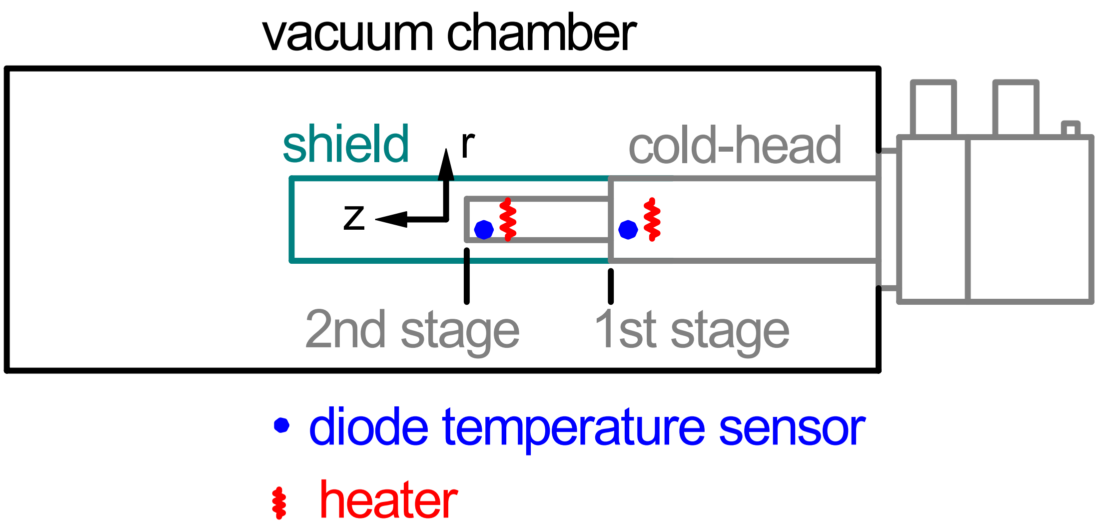

Figure 2: Schematic of the load mapping apparatus.

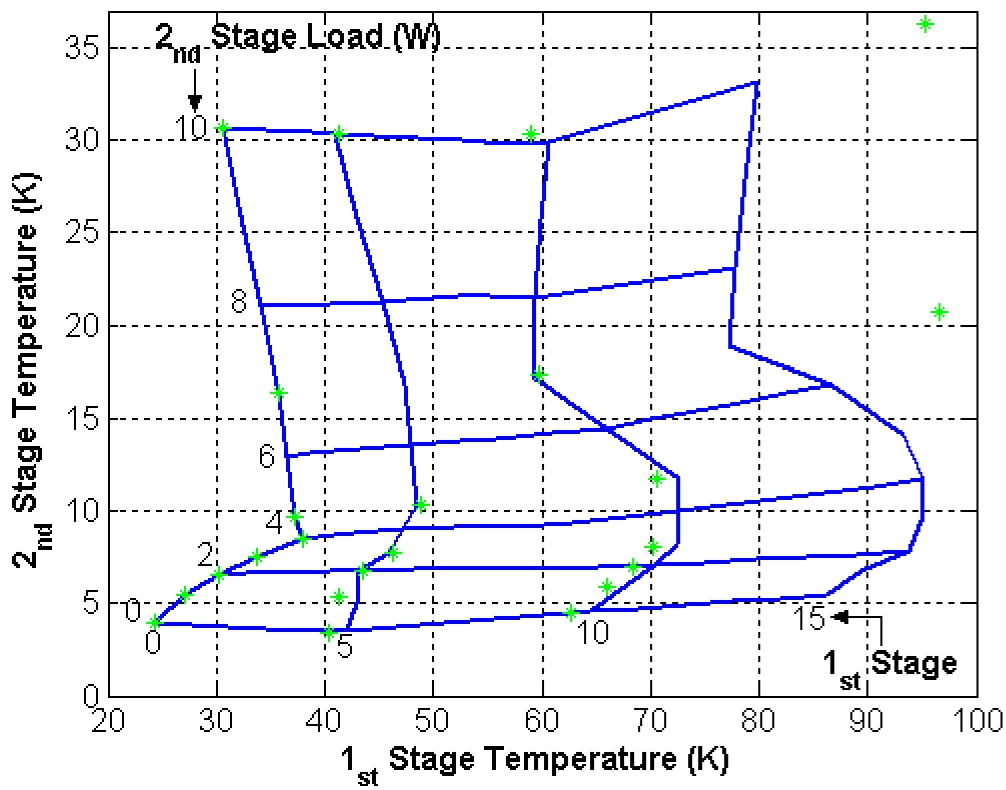

Figure 3: Measurement points (*) used to interpolate a load map (—).

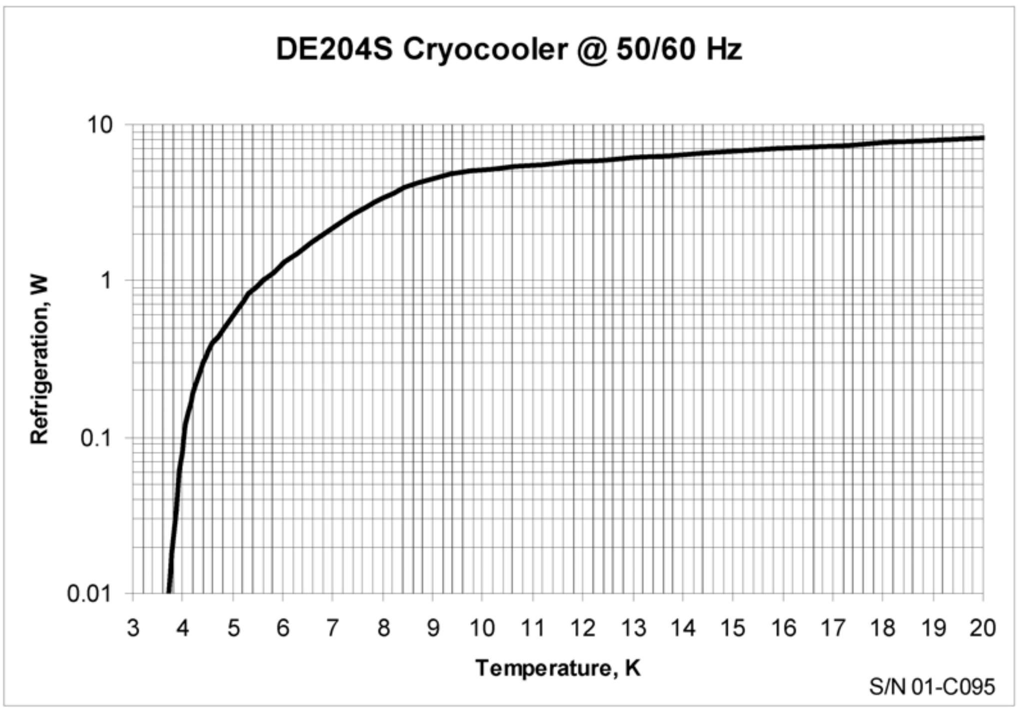

Note : Typical results - no attachments

Figure 4: Typical 2nd stage refrigeration as reported by ARS, Inc.

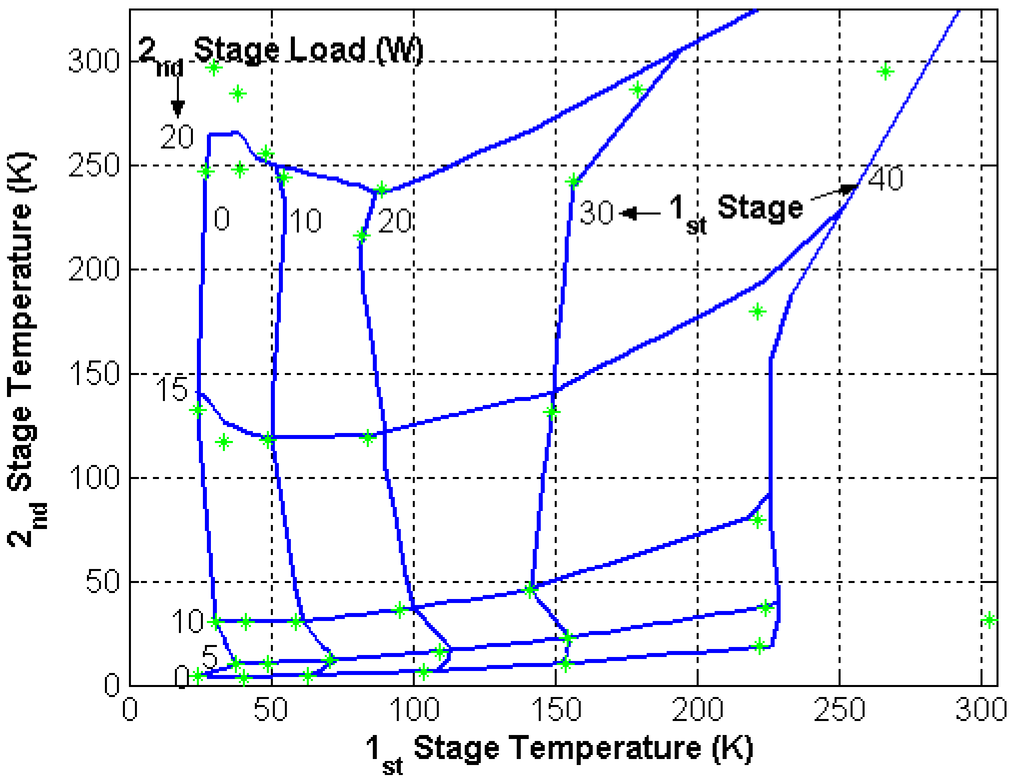

Figure 5: Load map extended close to room-temperature for both stages.

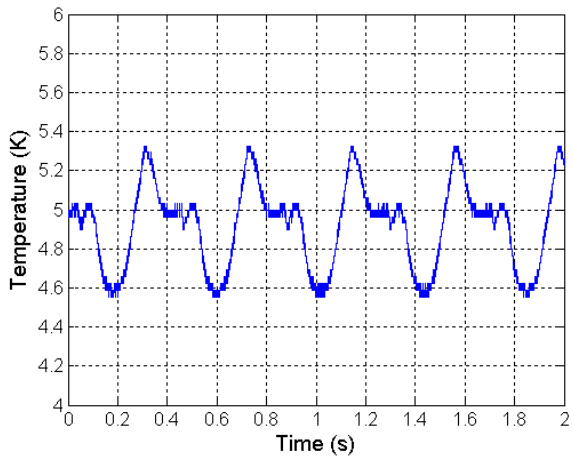

(a)

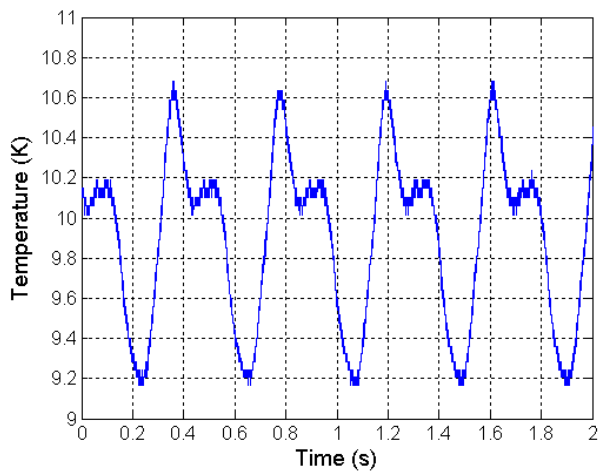

(b)

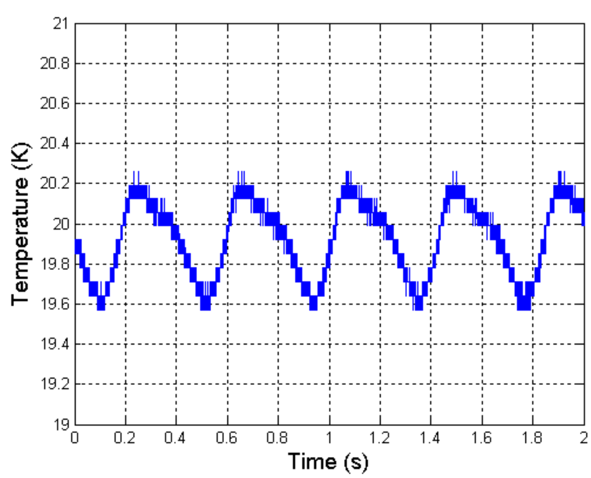

(c)

Figure 6: Temperature response at (a) ≈5K, (b) ≈10K, and (c) ≈20K.

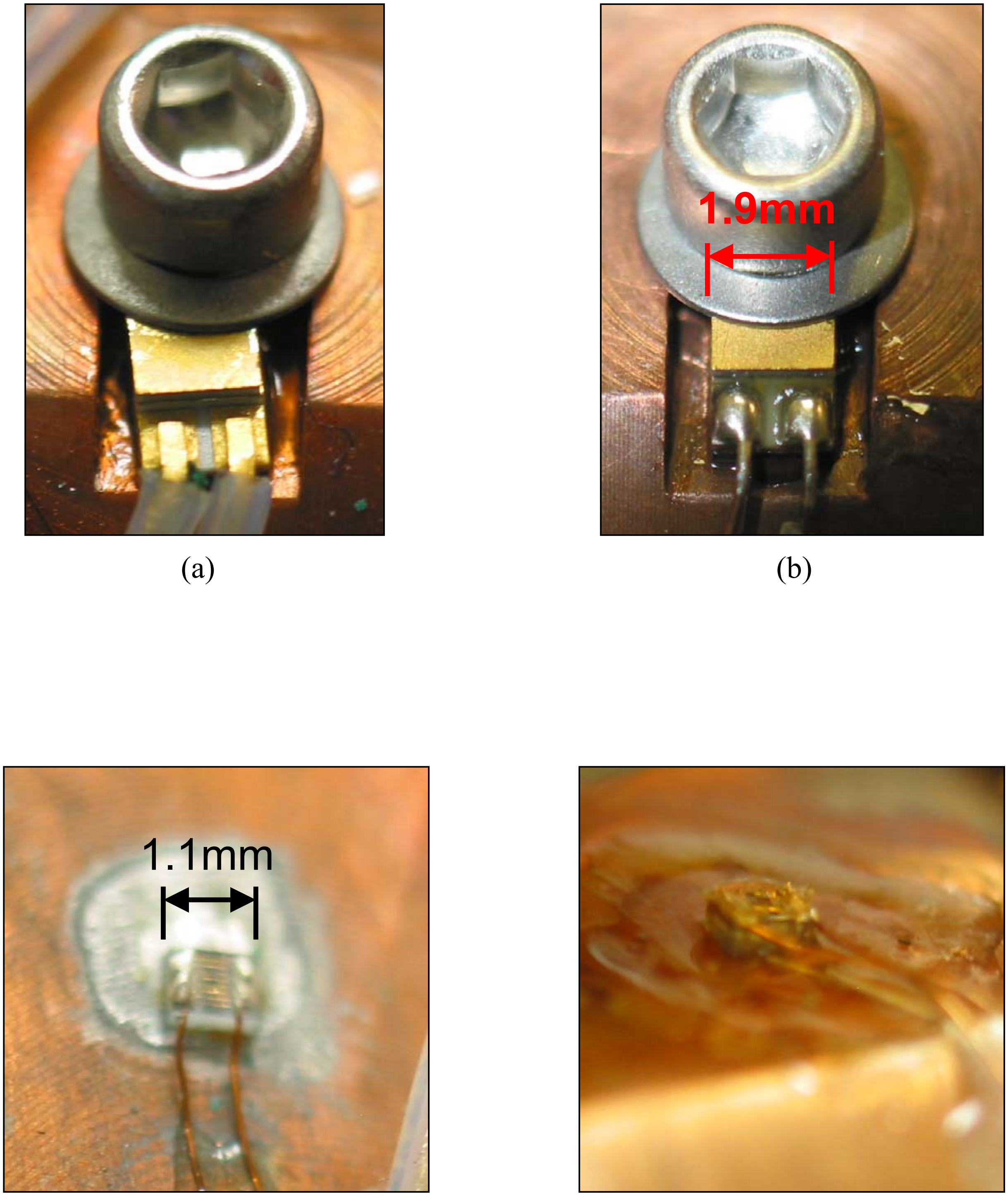

Figure 7: Photographs of sensor packaging and mounting schemes: (a) silicon diode in a hermetic package and clamped, (b) a Cernox chip in a hermetic package and clamped, (c) a bare Cernox chip that was soldered, and (d) a bare Cernox chip that was adhered with varnish.

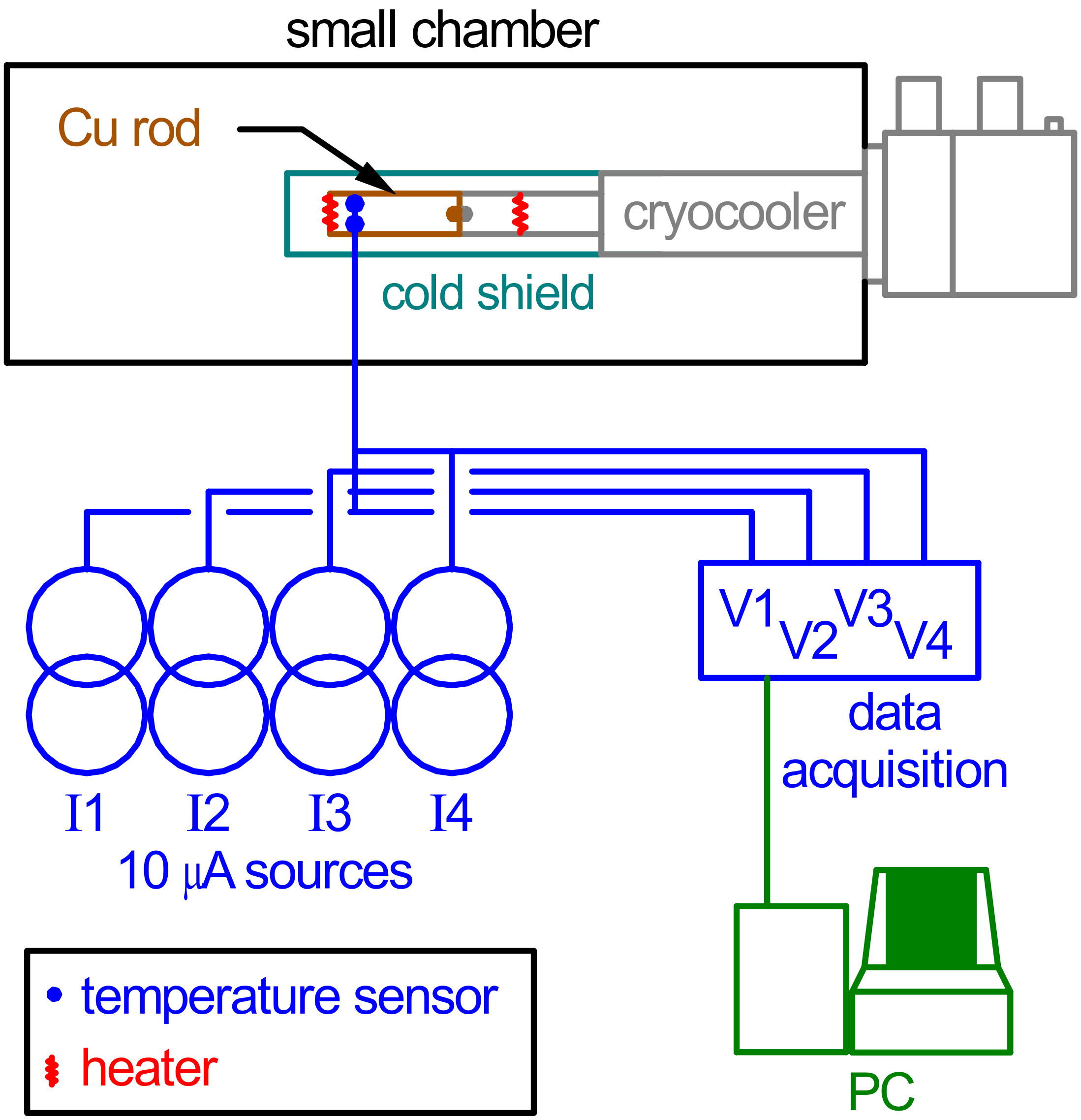

Figure 8: System used for comparing sensor configurations.

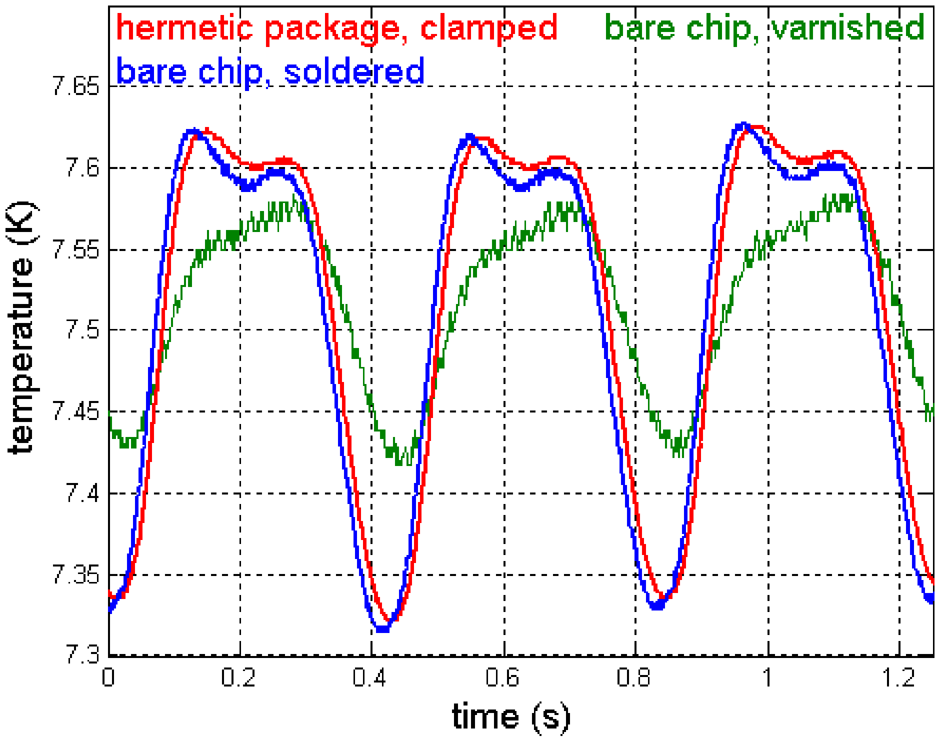

Figure 9: Comparison of the Cernox temperature responses at ≈7.5K.

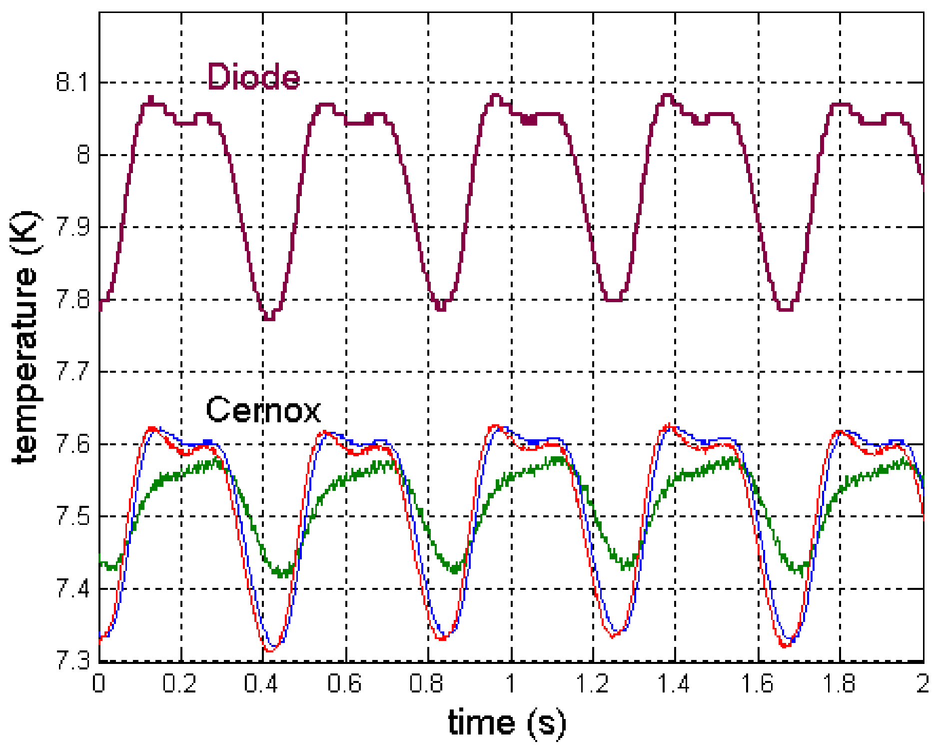

Figure 10: Comparison of the Cernox sensors and the diode sensor temperature response at ≈7.5K.

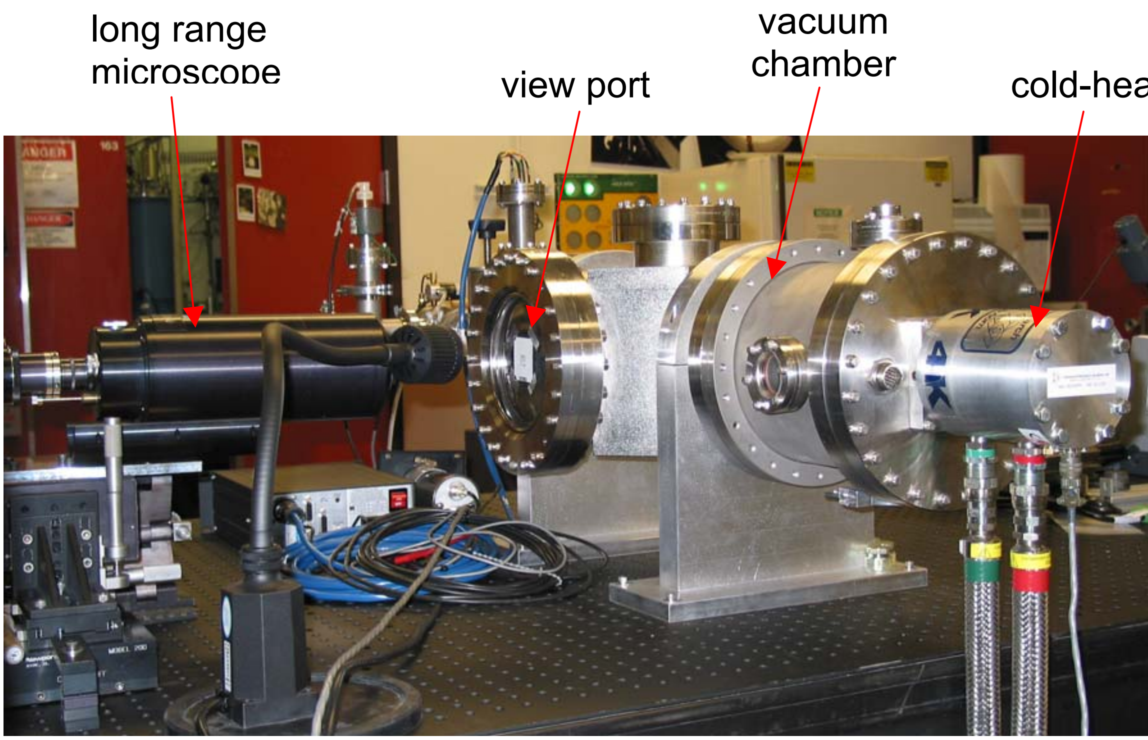

Figure 11: Apparatus for measuring 2nd stage heat station deflections.